UV Light Degradation of Polylactic Acid Kickstarts Enzymatic Hydrolysis

Margaret H. Brown, Thomas D. Badzinski, Elizabeth Pardoe, Molly Ehlebracht and Melissa A.

5 Maurer-Jones*

Department of Chemistry and Biochemistry, University of Minnesota Duluth, 1038 University Dr, Duluth, MN 55812

*Corresponding author (<u>maujones@d.umn.edu</u>)

ABSTRACT

Polylactic acid (PLA) and bioplastics alike have a designed degradability to avoid the environmental buildup petro plastics have created. Yet, this designed biotic-degradation has typically been characterized in ideal conditions. This study seeks to relate the abiotic to the biotic degradation of PLA to accurately represent the degradation pathways bioplastics will encounter supposing their improper disposal in the environment. Enzymatic hydrolysis was used to study the biodegradation of PLA with varying stages of photo-aging. Utilizing a fluorescent tag to follow enzyme hydrolysis, it was determined that increasing amounts of irradiation yielded greater amounts of total enzymatic hydrolysis by proteinase K after 8 h of enzyme incubation. While photo-aging of the polymers causes minimal changes in chemistry and increasing amounts of crystallinity, the trends in biotic degradation appear to primarily be driven by photo-induced reduction in molecular weight. The relationship between photo-aging and enzyme hydrolysis appears to be independent of enzyme type, though commercial product degradation may be impacted by the presence of additives. Overall, this work reveals the importance of characterizing the biodegradation with relevant samples that ultimately can inform optimization of production and disposal.

KEYWORDS: polylactic acid, biodegradability, abiotic degradation, UV light, enzymatic hydrolysis

INTRODUCTION

Given the critical role plastics play in daily life, biodegradable polymers seek to combat the environmental problems that have been caused through mismanagement of petro-plastic waste. Bioplastics like polylactic acid (PLA) offer a promising alternative to petro-plastics because it is expected that their designed biodegradability will give another pathway of breakdown and disposal that are not afforded to the legacy polymer products. The popularity of such innovative polymers continues to grow with a projected production rate of over 6.3 million tons in 2027. Of these 6.3 million tons, 37.9% of production is expected to be PLA and have a

market value of over 2.2 billion USD.¹⁻³ As the bioplastic market expands it becomes imperative to ensure these new materials do not add to current pollution problems.

Should they enter the environment unintentionally, PLA weathers through chemical and physical processes. Photo-degradation is noted as the most common abiotic degradation driving force. In PLA, the effects of photodegradation include an increase in brittleness, crystallinity, hydrophilicity, and a reduction of molecular weight. Similar changes and trends have been observed in petroplastics. When applied to biodegradation of petroplastics, the relative crystallinity drives the polymer's ability to biodegrade. That is, crystallinity prevents the adsorption of microorganisms to polymer surfaces, reducing the biodegradation capabilities. P-11 Thus the weathering induced changes in properties greatly affect the polymer's ability to degrade.

Currently, much of the work characterizing the biodegradability of these new materials occur under the most ideal conditions, ^{9, 12-17} and do not typically account for changes to the polymer throughout its use and disposal. The designed degradability of biodegradable plastics can be delayed or altered by the makeup of commercial products (i.e., the use of additives) or its state of degradation. ¹⁸⁻²¹ Ultimately, this could cause more waste accumulation in the environment for which mitigation techniques are currently no different than petroplastic waste. Therefore, it is critical to consider end-of-life conditions plastic products experience, including additives and the state of weathering of the plastics, that could prevent wide scale commercial integration of bioplastics.

Enzyme hydrolysis provides a tool to investigate the effects polymer weathering has on the designed biodegradability of PLA. As the first step in total biodegradation of plastics, enzymatic hydrolysis results in the cleavage of polymers chains into monomers, dimers, and oligomers capable of being mineralized by microorganisms.²²⁻²³ Given the importance of enzymatic hydrolysis for total biodegradation, it is the process this study tracks to evaluate biotic degradation. Further, measuring enzymatic hydrolysis is the prevailing approach to evaluate biodegradability within the literature.^{9, 20-21, 24-27} However, there exists a gap within current knowledge of environmental degradation that encapsulates both abiotic and biotic factors. Herein, this study demonstrates the relationship between photo- and biodegradation in PLA and reveals that rather than crystallinity hindering biodegradation, decreases in polymer molecular

weight boost biodegradation with photo-aging. Ultimately, biodegradation measurements indicate photo-weathering promotes the enzymatic hydrolysis in aged PLA samples.

MATERIALS AND METHODS

Plastic and Plastic Preparation

Poly-*L*-lactic acid (PLLA) thin film samples used in this study were 50 μm thick (Goodfellow; Huntingdon, GB). PLLA granules of different molecular weights were purchased from Polysciences (Warington, PA). To study the effects of additives, commercially available plastic cutlery (World Centric) and common commercial additives were used. In experimentation, plastic cutlery was used as-is. Additive doped polymers were pristine PLLA samples spiked with commercially relevant amounts of titanium dioxide (TiO₂; 4% w/w; a coloring agent) (CAS#13463-67-7, Bis (2,2,6,6-tetramethyl-4-piperidyl) (3% w/w; a UV stabilizer) (CAS#52829), or talc (11% w/w; a bulking agent) (CAS#14807-96-6). Prior to experiments, polymer thin film samples soaked for 24 h in each of hexanes (CAS#110-54-3), followed by methanol (CAS#67-56-1), and then doubly distilled water to remove unpolymerized monomers/oligomers or processing additives. This leaching process was not employed for cutlery or molecular weight standards.

Accelerated UV degradation was performed in a Rayonet merry-go-round photochemical reactor (Southern New England Ultraviolet Co.; Branford, CT) by irradiating films on both sides for various time periods with 16 Hg-vapor lamps (SNE Ultraviolet Co RMR-2537A; Bamford, CT) emitting photons centered at 300 nm light. PLLA was aged for 0, 1, 2, 3, 4, 8, and 24 h per side in this accelerated artificial fashion to produce equivalent natural aging byproducts.⁸

Enzymatic Hydrolysis Tracking with Fluorescence Spectroscopy

To quantitatively track the enzymatic hydrolysis of aged PLLA samples, a fluorogenic-labeling method was used based on a previous study. Briefly, samples were prepared in a chloroform solution with PLLA (2% (w/w)) and fluorescein dilaurate (0.002% (w/w) (FDL; CAS#7308-90-9) (Sigma Aldrich). Samples with additives were cast with the same PLLA and FDL concentration, keeping the amount of PLLA consistent in the cast between the different

additives. Samples were cast into the bottom of 10 mm Starna Cells quartz cuvettes (Atascadero, CA) and allowed to dry completely for a minimum of 12 h. This results in approximately a 30 µm thick film at the bottom of the cuvette. Samples were prepared in quadruplicate to produce triplicate enzymatic hydrolysis measurements along with a reference. Prior to casting the doped-polymer solutions, cuvettes were cleaned in Hellmanex III (Z805939) to ensure protein did not bind to the glass surface during experimentation.

Proteinase K (CAS# 39450-01-6) was purchased from Research Products International (Mt. Prospect, IL) and used at a concentration of 30 μ M in Tris HCl (CAS# 1185-53-1) at a pH 7.5 for all samples. The concentration of enzyme was chosen based on experimentation to optimize enzyme binding as described in the supporting information (Supporting Information Figure S1). Experiments were run in batches at 37°C. The protein solution was added to the cuvette immediately before the start of fluorescence measurements.

Fluorescence measurements were taken on a Horiba Fluoromax-4 Spectrofluorometer (Horiba Scientific; Edison, NJ) with an attached Quantum Northwest Temperature Control Turret with 4 cuvette slots (Liberty Lake, WA) and Koolance EXT-440 Liquid Cooling System (Auburn, WA). Excitation was 485 nm and emission spectra were collected from 500-650 nm with a 4 nm slit width for both excitation and emission. Measurements were taken in triplicate every 5 min over the span of 8 h. An additional reference cuvette with doped-PLLA with only Tris HCL buffer was run concurrently with enzyme samples.

To analyze the fluorescence data, the reference cuvette signal was subtracted from each sample cuvette to account for any auto-hydrolysis and release of the fluorogenic probe (See SI Figure S6 and S7). At lower levels of hydrolysis, fluorescence signal at 511 nm was used to convert into a concentration of fluorescein using a fluorescein calibration curve (SI Figure S5). When high concentrations of fluorescein were released, a bathochromic spectral shift was observed and calibration of the concentration of fluorescein was calibrated to the peak wavelength value (See SI Figure S3 and S4 for more information). The fluorescein concentration was converted into percent (%) ester bonds by comparing the amount of fluorescein, which was formed when 2 ester bonds per FDL molecule were cleaved, to the number of ester bonds within casted films. Ultimately, the values were converted into the amount of ester bonds broken in PLLA and a percent ester linkages broken by comparing to the total number of ester bonds in the cast PLLA. It should be noted that switching the calibration methods may have induced artifacts

in the observed hydrolysis rates. However, when comparing total ester bonds broken values between different polymer samples, we ensured the fluorescein concentrations, and thus the ester cleavage percent, were calculated with the same calibration methods, allowing us to evaluate trends of biodegradation between different sample types.

Attenuated Total Reflectance - Fourier Transform Infrared (ATR-FTIR) Spectroscopy

ATR-FTIR was performed on the samples to characterize the molecular structures on the polymer surface. A Nicolet iS50 (Thermo Fisher Scientific; Waltham, MA) with diamond ATR cell was used. Spectra measurements were collected at a minimum of 3 locations per sample. Each spectrum was an average 64 scans with a 4 cm⁻¹ resolution. Analysis of the carbonyl and hydroxyl bands in the spectra is a measure of the degree of weathering, as both are well established to grow with photodegradation.^{4,11} To quantify the carbonyl band, ATR-FTIR measurements of aged PLLA samples were analyzed using Igor Pro 8.04 (WaveMetrics; Portland, OR) software, individually analyzing the spectra carbonyl absorption band area (1730-1800 cm⁻¹) and normalized to a reference band area (~1455 cm⁻¹). This ratio generated a single value known as a carbonyl index. Similarly, a hydroxyl index was calculated using the hydroxyl absorption band area (3230-3700 cm⁻¹) and reference band area. The analysis was conducted on each triplicate measurement for plastic samples and the mean and standard deviation between trials was calculated.

Differential Scanning Calorimetry (DSC)

DSC measurements were conducted using an established method for PLLA on a TA Instruments DSC 250+ calorimeter (New Castle, DE, USA). Samples were analyzed in triplicate using between 5 and 10 mg of thin film sample in each Tzero pans. Samples were analyzed using a heat-cool-heat cycle, with the temperatures ranging from 25-170°C at a ramp rate of 10°C/min. Analysis was conducted on the first heating of the samples. Heat flow measurements were automatically normalized by sample mass on collecting. The enthalpy of melting was used to determine the bulk crystallinity where enthalpy was normalized to the enthalpy of melting a 100% crystalline sample (93.6 J/g) to calculate the percent crystallinity of the sample.²⁹

Scanning Electron Microscopy

A Hitachi TM3030 Tabletop Plus scanning electron microscope was used to observe the surface of PLLA upon enzymatic hydrolysis. Samples were mounted with carbon tape and imaged uncoated at 5 kV accelerating voltage.

RESULTS AND DISCUSSION

Aging of PLLA Promotes Enzymatic Hydrolysis

Figure 1 shows the enzymatic hydrolysis, monitored for 8 h, of aged PLLA. As the irradiation time of the plastic increases, the overall number of ester bonds broken over the course of study increases from 5.4 to 10.3% (SI Table S1). There appears to be different initial rates where 4 h is fastest and pristine is slowest, but mid-range aging does not stay on trend (3 h is slower initially than 2 h). That said, the hydrolysis results maintain the trend where increasing aging causes greater enzymatic breakdown upon 8 h. This is further demonstrated with samples aged for 8 and 24 h (SI Figure S8 and Table S1), where 24 h aging reaches up to 80% hydrolysis. We fit the data to reaction rate kinetics (SI Table S3); however, we also sought to perform experiments to determine if the cause of the changing rates in hydrolysis over the 8 h was the result of changing catalytic behavior of the enzyme (SI Figure S10 and S11). With fresh enzyme solution, hydrolysis continued, which indicates that the total values measured in Figure 1 are not the total amount that could be hydrolyzed. To confirm, PLLA samples of unaged and aged (4h irradiation) were refreshed with enzyme over the course of 3 days. Using mass measurements, it was determined that aged PLLA hydrolyzed more than unaged. Pristine PLLA exhibited a 11.00% mass loss with aged PLLA demonstrating a 14.38% mass loss.

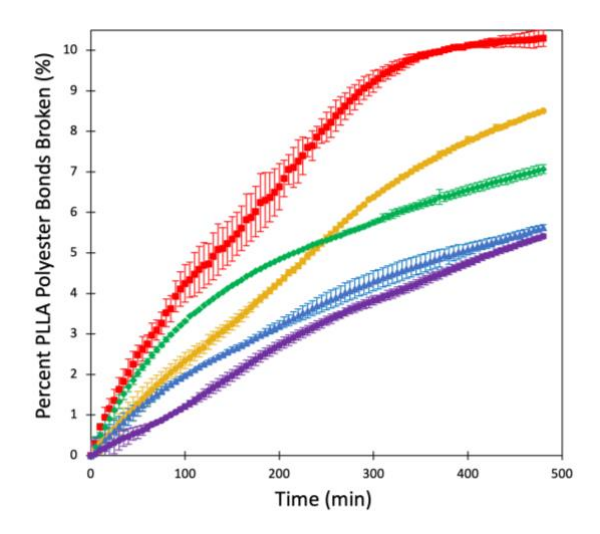


Figure 1: Percentage of PLLA polyester bonds broken over time of pristine, 1 h, 2 h, 3 h, and 4 h irradiated PLLA. Markers represent the average of triplicate values with error bars the standard deviation.

Previous work with PLLA suggests that aging should hinder enzymatic hydrolysis. Cai et al., reported the physical aging of PLLA utilizing thermal degradation hindered total biotic degradation. These results were correlated to the accompanied increase in crystallinity, a main characteristic change during PLA thermal degradation thought to be caused by a reduction in molecular weight. Our work reveals that UV degradation has an opposite effect where enzymatic hydrolysis is promoted by this aging. This phenomenon has been reported previously by Salac et al., who utilized compost to biodegrade photodegraded PLA. The study noted that after 90 days both non and photodegraded samples reached full mineralization, but that non-irradiated samples lagged at starting stages of biotic degradation. To understand the transformations driving the observed changes in enzyme hydrolysis, we characterized the material properties.

Characterizing Aged PLLA Films

In order to capture any chemical changes occurring as the result of photo-aging, ATR-FTIR analysis of PLLA films were probed to characterize carbonyl and hydroxyl indices. Increases in either index serve as markers for degradation.^{4, 11} However, our FTIR analysis proved to be insensitive to significant changes in chemistry, likely because PLA contains oxygen groups intrinsic to its structure that make small changes in these moieties difficult to observe. Figure 2A shows the hydroxyl and carbonyl index in the polymers upon irradiation. While there appears to be a slight decreasing trend in the carbonyl index, ANOVA tests revealed no

statistically significant difference in either index with increased irradiation. This result is not novel, Salac et al., and more recently Companaro et al., reported no FTIR discernible changes in photodegraded PLLA, respectively. ^{21, 25} Similarly, carbonyl and hydroxyl indices were quantified following enzyme exposure and again no statistically significant changes were observed with photoaging, though the enzyme caused differences from the non-enzyme exposed samples (SI Figure S12).

218

212

213

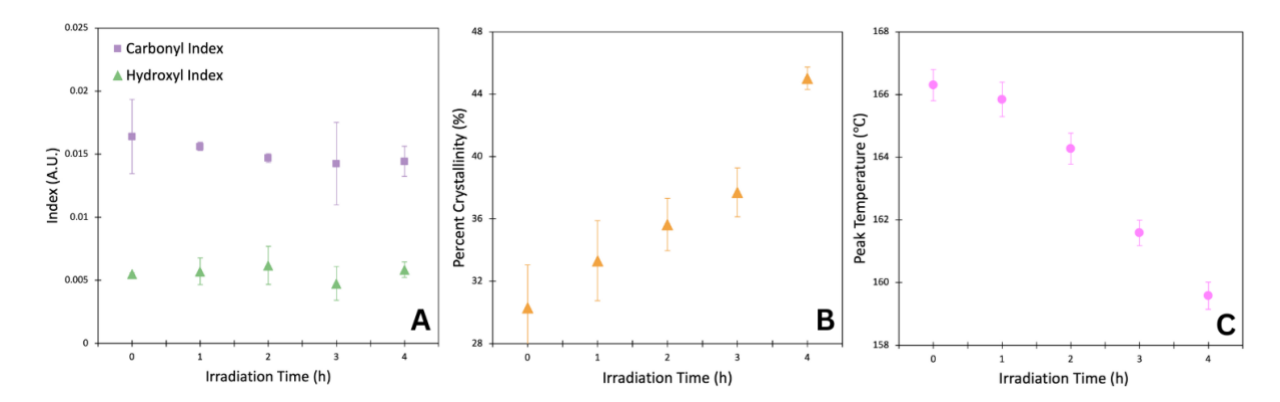
214

215

216

217

219



220 221

Figure 2: (A) Carbonyl and hydroxyl indices of irradiated PLLA samples. Markers represent the average of triplicate values with error bars the standard deviation. (B) Percent bulk crystallinity (%) of irradiated PLLA samples. (C) Peak temperature °C of irradiated PLLA samples from DSC thermograms.

223 224

225

226

227

228

229

230

231

232

222

We further investigated the changes in crystallinity to understand its role in total decomposition or potentially its impact on initial rates of irradiated samples. Bulk crystallinity measurements as determined from the DSC data (SI Figure S13) revealed an increase in crystallinity with greater levels of aging (Figure 2B). It has been readily determined that highly crystalline polymers, specifically PLLA, inhibit biotic degradation. 9, 26-27 Since the observed trend in our photodegraded samples has increasing crystallinity, this indicates that the susceptibility of UV light degraded PLA to enzymatic hydrolysis must be influenced by a different material property (e.g., density, molecular weight, tensile strength).

233 Peak temperature in the DSC thermograms is an established method for comparison of molecular weights.³⁰ Further, it has been readily demonstrated that photodegradation causes a 234 235 reduction in molecular weight, and separately that lower molecular weight PLLA degrades at a 236 faster rate than their high molecular weight counterparts.³¹ Figure 2C illustrates that increasing UV exposure causes a decrease in peak temperature, indicating reduction in molecular weight. 237

Ultimately, these results indicate that changes in molecular weight play an integral role in the enzymatic hydrolysis and aging trends demonstrated above. To confirm DSC peak temperature measurements could accurately detect changes within molecular weight, PLLA molecular weight standards were analyzed with DSC and revealed decreasing peak temperatures with decreased molecular weight (SI Figure S14 and Table S4). Taking the materials characterization together, photo-aging causes minor changes in the PLLA chemistry and the observed changes in crystallinity should have caused decreased enzyme hydrolysis based on the literature; 9, 26-27 therefore, we concluded that the photochemically-induced decrease in molecular weight is the primary transformation dictating the efficiency of the enzymatic hydrolysis of aged PLLA.

SEM was performed to observe any changes happening to the polymer surface upon exposure to enzyme. Pristine PLLA exposed to enzyme revealed a branching pattern, while aged PLLA revealed no distinctive landmarks (Figure 3). Taken together with the hydrolysis and polymer characterization results reported above, we concluded that UV degradation causes lower molecular weight chains more homogeneously on the polymer surface and that this uniformity allows for more areas in which the enzyme can attack in aged polymers.

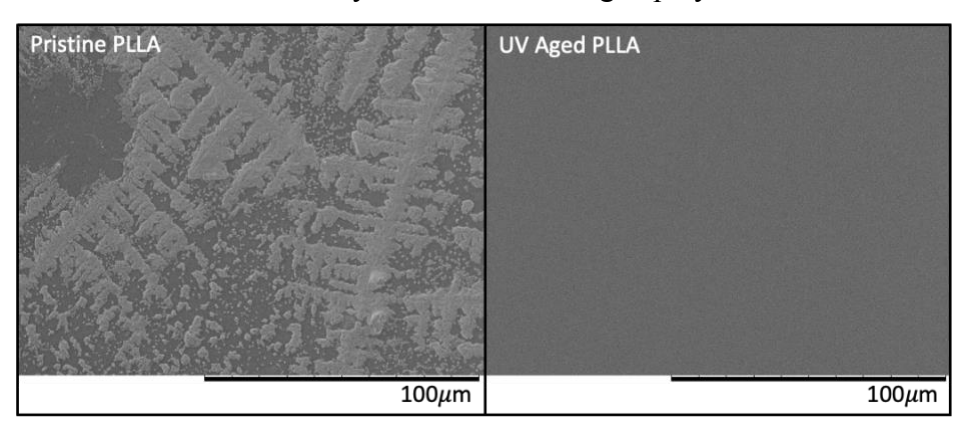


Figure 3: SEM Imaging of pristine and aged (8 h UV) PLLA. These are representative images of n=1 sample per condition with >20 images taken per sample.

Enzyme Hydrolysis of Molecular Weight Standards

With DSC observed reduction in molecular weight as a result of aging, we sought to confirm our fluorescence method could accurately track increased enzymatic hydrolysis of lower molecular weight samples, a trend established in the literature. ¹² Our fluorogenic probe was doped into PLLA molecular weight standards (average molecular weights of 2, 50, 90, and 300 kDa) (Figure S8). Figure 4 demonstrates that decreasing the molecular weight yields greater

amounts of enzymatic hydrolysis over 8 h, confirming that molecular weight is tied to the ability of PLLA to biodegrade.



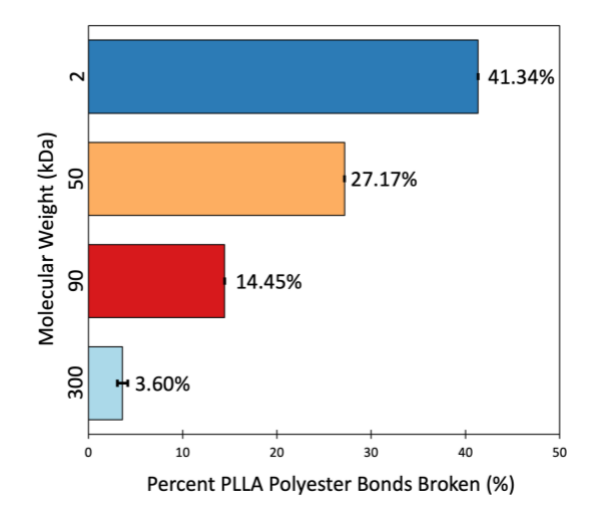
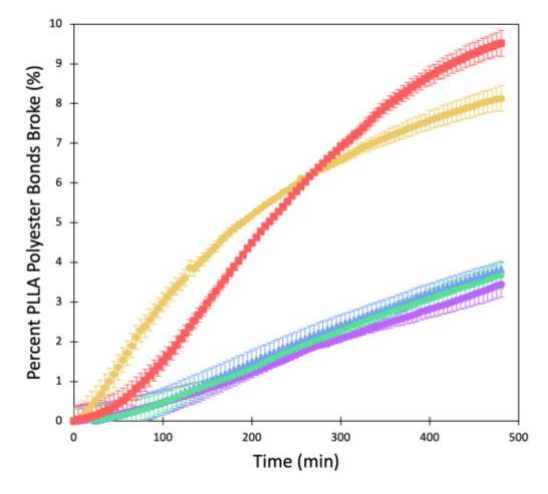


Figure 4: Total percentage of PLLA polyester bonds broken after 8 h of proteinase K exposure in 2, 50, 90, and 300 kDa PLLA molecular weight standards. Values represent the average of 3 replicate samples and error bars as standard deviations.

Trends Utilizing Other Enzymes

Our experimentation above used an ideal system for the biotic degradation of PLLA as proteinase K is the leading enzyme for the catalysis of PLLA enzymatic hydrolysis. 32-33 To determine if the trends demonstrated are more generalizable, the biodegradability experiments were repeated utilizing another esterase, triacylglycerol lipase. Lipases are present in a high majority of living organisms, with a large number of fungi also producing lipases. 34 Tokiwa et al., demonstrated the ability of lipase to degrade synthetic polyesters and Alejandra et al., confirmed lipase's degradation capabilities in poly(3-hydroxybutyrate-co-4-hydroxybutyrate). 35-36 Ultimately, lipase is a readily available enzyme and shown to degrade polyesters. 37-38 Figure 5 shows that lipase induces a near identical trend in enzymatic hydrolysis as proteinase K. The presence of the identical catalytic triad in both lipase and proteinase K may be the cause for the similar response. That is, both proteinase K and lipase exhibit the 'catalytic triad of aspartic acid (Asp), histidine (His), and serine (Ser). 39 The catalytic triad catalyzes the nucleophilic attack on carbonyl carbons in esters using the active site serine. 38 While further work exploring wider enzyme structures may yield varied biodegradation capability, it is still important that both hydrolases have promoted activity on UV degraded polymers irrespective of individual enzymes.



288 289

Figure 5: Percentage of PLLA polyester bonds broken over time of pristine, 1 h, 2 h, 3 h, and 4 h irradiated PLLA utilizing lipase. Markers represent the average of triplicate values with error bars the standard deviation.

291292

293

290

Effects of Additives on Enzymatic Hydrolysis

294295

296

297

298

299

300

304

305

306

307

308

309

310

311

samples, such as plastics that are exposed to abiotic factors such as photodegradation, it is also important to study the effects of realistic commercial polymer products that include additives.

To continue to build on our understanding of the biotic breakdown of relevant polymer

Initially, to determine if enzyme hydrolysis is impacted by additives, PLA compostable cutlery

was studied using the fluorescence methodology. PLA cutlery degraded close to 100% after 4 h, greater than the 12% observed with the 2 kDa PLLA molecular weight standard that had the

closest DSC peak melting temperature (158°C) compared to the cutlery (164°C) (SI Figure 15).

It was determined gravimetrically that the cutlery was composed of 11% filler, which was reported by the manufacturer to primarily be talc. Further experiments were performed by systematically changing additives that were doped into pristine PLLA (Figure 6A). Similarly, to

the PLA cutlery sample, the presence of additives kickstarts enzymatic hydrolysis in initial

stages of degradation. The three additives chosen were titanium dioxide (TiO₂; a coloring agent)

Bis (2,2,6,6-tetramethyl-4-piperidyl) a UV stabilizer) and talc (a bulking agent) and were doped

at commercially relevant weight percentages. In studies investigating the effects of titanium

dioxide (TiO₂) as an additive in the biodegradation of PLA, it was found to promote the rate of

PLA degradation because it increased the ability for water to penetrate the PLA/TiO₂ mixtures.⁴¹⁻

⁴² Conversely for talc, Li et al., reported talc in PLA as a successful nucleating agent, increasing

the crystallinity of PLA,⁴³ which should decrease biodegradability as others observed in

industrial composting conditions.^{20,44} Because our results contradicted previous studies relating the presence of talc to biodegradation, the fluorescent experiments were conducted at varying w/w percentages of talc to PLLA (Figure 6B). As shown, the presence of talc in all weight percentages increased enzymatic hydrolysis over a 4 h period. Interestingly, the middle point of 5.5% (w/w) of talc in PLLA resulted in the greatest total number of polyester bonds broken, indicating the concentration of additives is ultimately important in the biodegradation of PLLA. However, with a clear bump in degradation from talc presence alone it is clear that these additives affect PLLA properties, thus boosting enzyme hydrolysis. Overall, the molecule and pigment additives studied here likely disrupt the packing of the polymer backbones, yielding more amorphous PLLA with better solvent/enzyme access allowing for greater biodegradation.

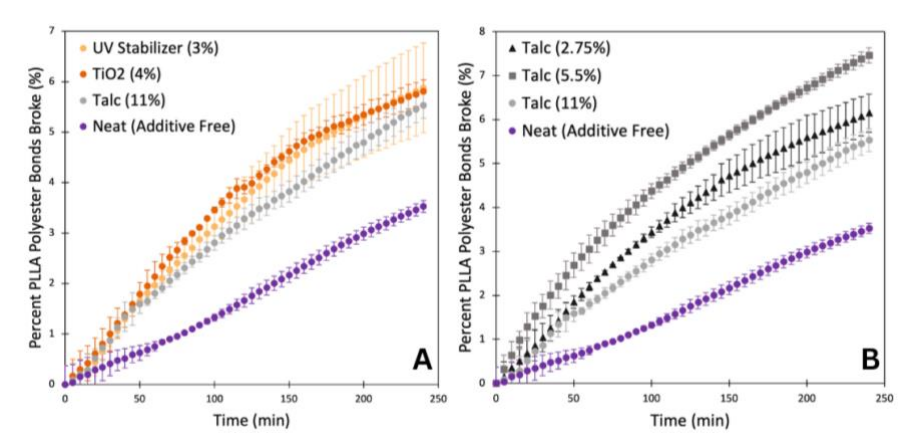


Figure 6: (**A**) Percentage of PLLA polyester bonds broken over time of pristine PLLA doped with 3% w/w Bis (2,2,6,6-tetramethyl-4-piperidyl) (UV Stabilizer), 4% w/w titanium dioxide (TiO2), and 11% w/w Talc compared to a neat (additive free) PLLA. Markers represent the average of triplicate values with error bars the standard deviation. (**B**) Percentage of PLLA polyester bonds broken over time of pristine PLLA doped with 2.75, 5.5, and 11% w/w Talc compared to a neat (additive free) PLLA. Markers represent the average of triplicate values with error bars the standard deviation.

CONCLUSIONS

Our study demonstrated that total enzyme hydrolysis was heightened by environmentally relevant treatment where UV degradation of PLA causes an increase in biodegradation. This relationship is the result of reduced molecular weight caused by photoaging. Further, the presence of additives serves a similar purpose in altering the packing of the polymer to allow for expedited biodegradation. Ultimately, this study serves to identify the effects of environmentally relevant degradability on waste PLLA to better inform its design and disposal. As plastic

338 pollution continues to grow, it is necessary to evaluate these assumptions in follow-up studies to 339 evaluate, consolidate, and expand the discussed results.

340 341

SUPPORTING INFORMATION:

Methods to optimize enzyme concentration, calibrating fluorescence dilaurate with fluorescence spectroscopy, tables of hydrolysis quantification values, hydrolysis curves of standards, enzyme activity assay data and discussion, table of reaction rate fits, FTIR polymer analysis, DSC thermograms and melting point analysis, commercial PLA product enzyme hydrolysis data.

345 346 347

348

349

350

351

342

343

344

ACKNOWLEDGEMENTS

Financial support for this study was provided by NSF Center for Sustainable Polymers (CHE-1901635), the Warren F. Davis Chair in Chemistry Endowment fund, and the Department of Chemistry and Biochemistry at University of Minnesota Duluth in the form of a teaching assistantship to MHB and access to the fluorometer. The authors also acknowledge Adele 352 Kleppers and Dr. ChanLan Chun at the Natural Resources Research Institute for procurement of 353 SEM images.

354 355

REFERENCES

356 357

358

359

360

361

362

363

364

365

366

367 368

369

370 371

372

373

374

375

376

377 378

- 1. Annual production of plastics worldwide from 1950 to 2021. https://www.statista.com/statistics/282732/global-production-of-plastics-since-1950/ (accessed 2023-01-29).
- 2. Polylactic Acid Market Size 2023 2030. https://www.grandviewresearch.com/industryanalysis/polylactic-acid-pla-market (accessed 2022-04-04).
- 3. Poly Lactic Acid (Global Forecast to 2028). https://www.marketsandmarkets.com/Market-Reports/polylactic-acid-pla-market-29418964.html#:~:text=The%20global%20PLA%20market%20is,driving%20the%20ma rket%20for%20PLA. (accessed 2023-01-17).
- 4. Gewert, B.; Plassmann, M. M.; Macleod, M. Pathways for Degradation of Plastic Polymers Floating in the Marine Environment. Environmental Sciences: Processes and Impacts, 2015, 17, 1513–1521.
- 5. Tsuji, H.; Sugiyama, H.; Sato, Y. Photodegradation of Poly(Lactic Acid) Stereocomplex by UV-Irradiation. Journal of Polymers and the Environment 2012, 20 (3), 706–712.
- 6. Hebner, T. S.; Maurer-Jones, M. A. Characterizing Microplastic Size and Morphology of Photodegraded Polymers Placed in Simulated Moving Water Conditions. Environmental Science: Processes and Impacts 2020, 22 (2), 398–407.
- 7. Elmer-Dixon, M. M.; Fawcett, L. P.; Hinderliter, B. R.; Maurer-Jones, M. A. Could Superficial Chiral Nanostructures Be the Reason Polyethylene Yellows as It Ages? ACS Applied Polymer Materials 2022, 4 (9), 6458–6465.
- 8. Mundhenke, T. F.; Li, S. C.; Maurer-Jones, M. A. Photodegradation of Polyolefin Thin Films in Simulated Freshwater Conditions. Environmental Science: Processes and Impacts 2022, 24 (12), 2284–2293.
- 380 9. Cai, H.; Dave, V.; Gross, R. A.; McCarthy, S. P. Effects of Physical Aging, 381 Crystallinity, and Orientation on the Enzymatic Degradation of Poly(Lactic Acid). 382 Journal of Polymer Science, Part B: Polymer Physics 1996, 34 (16), 2701–2708.

10. Karamanlioglu, M.; Preziosi, R.; Robson, G. D. Abiotic and Biotic Environmental
 Degradation of the Bioplastic Polymer Poly(Lactic Acid): A Review. *Polymer Degradation and Stability*, 2017, 137, 122–130.

- 11. Chamas, A.; Moon, H.; Zheng, J.; Qiu, Y.; Tabassum, T.; Jang, J. H.; Abu-Omar, M.; Scott, S. L.; Suh, S. Degradation Rates of Plastics in the Environment. *ACS Sustainable Chemistry and Engineering* **2020**, *8* (9), 3494–3511.
 - 12. Chandra, R.; Rustgi, R. Biodegradable Polymers. *Prog. Polym. Sci*, 1998, 23, 1273–1335.
 - 13. Zaaba, N. F.; Jaafar, M. A Review on Degradation Mechanisms of Polylactic Acid: Hydrolytic, Photodegradative, Microbial, and Enzymatic Degradation. *Polymer Engineering and Science* **2020**, *60* (9), 2061–2075.
 - 14. Tokiwa, Y.; Calabia, B. P.; Ugwu, C. U.; Aiba, S. Biodegradability of Plastics. *International Journal of Molecular Sciences*, **2009**, *10*, 3722–3742.
 - 15. Ghosh, K.; Jones, B. H. Roadmap to Biodegradable Plastics-Current State and Research Needs. *ACS Sustainable Chemistry and Engineering*, **2021**, *9*, 6170–6187.
 - 16. Li, Y.; Qiang, Z.; Chen, X.; Ren, J. Understanding Thermal Decomposition Kinetics of Flame-Retardant Thermoset Polylactic Acid. *RSC Advances* **2019**, *9* (6), 3128–3139.
 - 17. Gleadall, A.; Pan, J.; Atkinson, H. A Simplified Theory of Crystallisation Induced by Polymer Chain Scissions for Biodegradable Polyesters. *Polymer Degradation and Stability* **2012**, *97* (9), 1616–1620.
 - 18. Ren, X. Biodegradable Plastics: A Solution or a Challenge? *Journal of Cleaner Production*, **2003**, *11*, 27–40.
 - 19. Karamanlioglu, M.; Robson, G. D. The Influence of Biotic and Abiotic Factors on the Rate of Degradation of Poly(Lactic) Acid (PLA) Coupons Buried in Compost and Soil. *Polymer Degradation and Stability* **2013**, *98* (10), 2063–2071.
 - 20. Lee, C.; Pang, M. M.; Koay, S. C.; Choo, H. L.; Tshai, K. Y. Talc Filled Polylactic-Acid Biobased Polymer Composites: Tensile, Thermal and Morphological Properties. *SN Applied Sciences* **2020**, *2* (3), 354.
 - 21. Salač, J.; Šerá, J.; Jurča, M.; Verney, V.; Marek, A. A.; Koutný, M. Photodegradation and Biodegradation of Poly(Lactic) Acid Containing Orotic Acid as a Nucleation Agent. *Materials* **2019**, *12* (3), 481.
 - 22. Amobonye, A.; Bhagwat, P.; Singh, S.; Pillai, S. Plastic Biodegradation: Frontline Microbes and Their Enzymes. *Science of the Total Environment* **2021**, 10, 143536.
 - 23. Maraveas, C. Production of Sustainable and Biodegradable Polymers from Agricultural Waste. Polymers, 2020, 12. https://doi.org/10.3390/POLYM12051127.
 - 24. Maraveas, C.; Kotzabasaki, M. I.; Bartzanas, T. Intelligent Technologies, Enzyme-Embedded and Microbial Degradation of Agricultural Plastics. AgriEngineering, 2023, 5, 85–111. https://doi.org/10.3390/agriengineering5010006.
- 25. Campanaro, A. L.; Simcik, M. F.; Maurer-Jones, M. A.; Penn, R. L. Sewage Sludge Induces Changes in the Surface Chemistry and Crystallinity of Polylactic Acid and Polyethylene Films. *Science of the Total Environment* **2023**, *890*, 164313.
- 424 26. MacDonald, R. T.; McCarthy, S. P.; Gross, R. A. Enzymatic Degradability of
 425 Poly(Lactide): Effects of Chain Stereochemistry and Material Crystallinity.
 426 *Macromolecules* 1996, 29, 7356-7361.

427 27. Tsuji, H.; Miyauchi, S. Enzymatic Hydrolysis of Poly(Lactide)s: Effects of Molecular
 428 Weight, L-Lactide Content, and Enantiomeric and Diastereoisomeric Polymer Blending.
 429 *Biomacromolecules* 2001, 2 (2), 597–604.

- 28. Zumstein, M. T.; Kohler, H. P. E.; McNeill, K.; Sander, M. High-Throughput Analysis of Enzymatic Hydrolysis of Biodegradable Polyesters by Monitoring Cohydrolysis of a Polyester-Embedded Fluorogenic Probe. *Environmental Science and Technology* **2017**, *51* (8), 4358–4367.
- 29. Song, L.; Li, Y.; Meng, X.; Wang, T.; Shi, Y.; Wang, Y.; Shi, S.; Liu, L. Crystallization, Structure and Significantly Improved Mechanical Properties of PLA/PPC Blends Compatibilized with PLA-PPC Copolymers Produced by Reactions Initiated with TBT or TDI. *Polymers* **2021**, *13* (19), 3245.
- 30. Ghijsels, A.; Waals, F. M. T. A. M. Differential Scanning Caolorimetry: A Powerful Tool for the Characterization of Thermoplastics. *Polymer Testing*, **1980**, *1*, 149–160.
- 31. Xie, Y. Y.; Park, J. S.; Kang, S. K. Studies on the Effect of Molecular Weight on Biodegradable Polymer Membrane. *International Journal of Bio-Science and Bio-Technology* **2016**, *8* (3), 315–322.
- 32. Williams, D. F. Enzymic Hydrolysis of Polylactic Acid. *Engineering in Medicine* **1981**, *10* (1), 5–7.
- 33. Jarerat, A.; Tokiwa, Y. Degradation of Poly(L-lactide) by a Fungus. *Macromole. Biosci.* **2001,** 1, 136-140.
- 34. Kumar, A.; Verma, V.; Dubey, V. K.; Srivastava, A.; Garg, S. K.; Singh, V. P.; Arora, P. K. Industrial Applications of Fungal Lipases: A Review. *Frontiers in Microbiology*, **2023**, *14*, 1142536.
- 35. Tokiwa, Y.; Suzuki, T. Hydrolysis of Polyesters by Lipases. *Nature* **1977**, *270* (3), 76-78
- 36. Alejandra, R. C.; Margarita, C. M.; Soledad, M. C. M. Enzymatic Degradation of Poly(3-Hydroxybutyrate) by a Commercial Lipase. *Polymer Degradation and Stability* **2012**, *97* (11), 2473–2476.
- 37. Kalita, N. K.; Hakkarainen, M. Triggering Degradation of Cellulose Acetate by Embedded Enzymes: Accelerated Enzymatic Degradation and Biodegradation under Simulated Composting Conditions. *Biomacromolecules* **2023**, 24(7), 3290-3303.
- 38. Kalita, N. K.; Hakkarainen, M. Integrating biodegradable polyesters in a circular economy. *Current Opinion in Green and Sustainable Chemistry* **2022**, 40, 100751.
- 39. Betzel, C.; Gourinath, S.; Kumar, P.; Kaur, P.; Perbandt, M.; Eschenburg, S.; Singh, T. P. Structure of a Serine Protease Proteinase K from Tritirachium Album Limber at 0.98 Å Resolution. *Biochemistry* **2001**, *40*, 3080–3088.
- 40. Lockridge, O.; Quinn, D. M. Esterases. In *Comprehensive Toxicology*; Elsevier, 2010; pp 243–273.x
- 41. Marra, A.; Cimmino, S.; Silvestre, C. Effect of TiO2 and ZnO on PLA Degradation in Various Media. *Advanced Material Science* **2017**, *2* (2), 1-8.
- 42. Luo, Y.; Lin, Z.; Guo, G. Biodegradation Assessment of Poly (Lactic Acid) Filled with
 Functionalized Titania Nanoparticles (PLA/TiO2) under Compost Conditions.
 Nanoscale Research Letters 2019, 14, 56.
- 43. Li, H.; Huneault, M. A. Effect of Nucleation and Plasticization on the Crystallization of Poly(Lactic Acid). Polymer **2007**, 48 (23), 6855–6866.

44. Tolga, S.; Kabasci, S.; Duhme, M. Progress of Disintegration of Polylactide (PLA)/Poly(Butylene Succinate) (PBS) Blends Containing Talc and Chalk Inorganic Fillers under Industrial Composting Conditions. *Polymers* **2021**, *23* (1), 1–19.

TOC Graphic

